Comparative assessment of TROPOMI and OMI formaldehyde observations against MAX-DOAS network column measurements.

Isabelle De Smedt[1], Gaia Pinardi[1], Corinne Vigouroux[1], Steven Compernolle[1], Alkis Bais[2], Nuria Benavent[3], Folkert Boersma[4,5], Ka-Lok Chan[6], Sebastian Donner[7], Kai-Uwe Eichmann[8], Pascal Hedelt[6], François Hendrick[1], Hitoshi Irie[9], Vinod Kumar[7], Jean-Christopher Lambert[1], Bavo Langerock[1], Christophe Lerot[1], Cheng Liu[10], Diego Loyola[6], Ankie Piters[4], Andreas Richter[8], Claudia Rivera Cárdenas[11], Fabian Romahn[6], Robert George Ryan[12,13], Vinayak Sinha[14], Nicolas Theys[1], Jonas Vlietinck[1], Thomas Wagner[7], Ting Wang[15], Huan Yu[1], Michel Van Roozendael[1].

Correspondence to: Isabelle De Smedt (isabelle.desmedt@aeronomie.be)

1. Royal Belgian Institute for Space Aeronomy (BIRA-IASB), Ringlaan 3, 1180 Uccle, Belgium.
2. Laboratory of Atmospheric Physics, Aristotle University of Thessaloniki (AUTH), Thessaloniki, Greece.
3. Department of Atmospheric Chemistry and Climate, Institute of Physical Chemistry Rocasolano (CSIC), Madrid, Spain.
4. Royal Netherlands Meteorological Institute (KNMI), De Bilt, the Netherlands.
5. Meteorology and Air Quality group, Wageningen University, the Netherlands.
6. Institut für Methodik der Fernerkundung (IMF), Deutsches Zentrum für Luft und Raumfahrt (DLR), Oberpfaffenhofen, Germany.
7. Max-Planck-Institut für Chemie (MPI-C), Mainz, Germany.
8. Institute of Environmental Physics, University of Bremen (IUP-B), Bremen, Germany.
9. Center for Environmental Remote Sensing, Chiba University (Chiba U), Chiba, Japan
10. Department of Precision Machinery and Precision Instrumentation, University of Science and Technology of China, Hefei, China.
11. Centro de Ciencias de la Atmósfera, Universidad Nacional Autónoma de México (UNAM), Mexico City, Mexico
12. School of Earth Sciences, The University of Melbourne, Melbourne, Australia
13. ARC Centre of Excellence for Climate System Science, Sydney, Australia
14. Department of Earth and Environmental Sciences, Indian Institute of Science Education and Research (IISER), Mohali, India
15. Institute of Atmospheric Physics, Chinese Academy of Sciences (CAS), Beijing, China

Supplementary figures

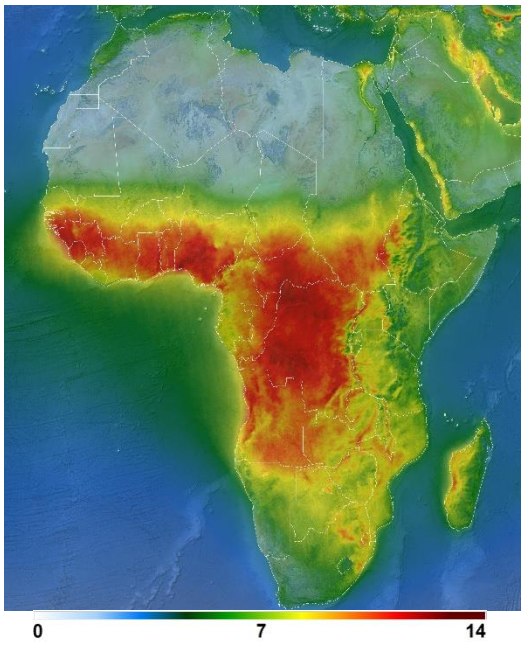

Africa (max.scale: $14x10^{15}$ molec.cm^{-2})

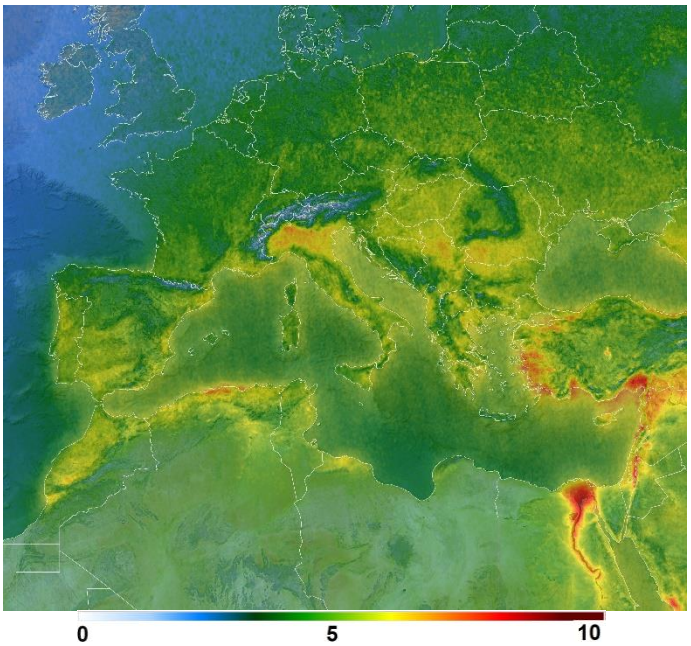

Europe (max.scale: $10x10^{15}$ molec.cm^{-2})

Figure S1: Multi-annual regional maps of TROPOMI HCHO tropospheric columns (March 2018 – February 2021), on a spatial grid of 0.05° in latitude and longitude. Observations are filtered using the provided qa_values>0.5. Modified Copernicus Sentinel-5P satellite data, OFFL L2 HCHO product, BIRA-IASB/DLR/ESA/EU.

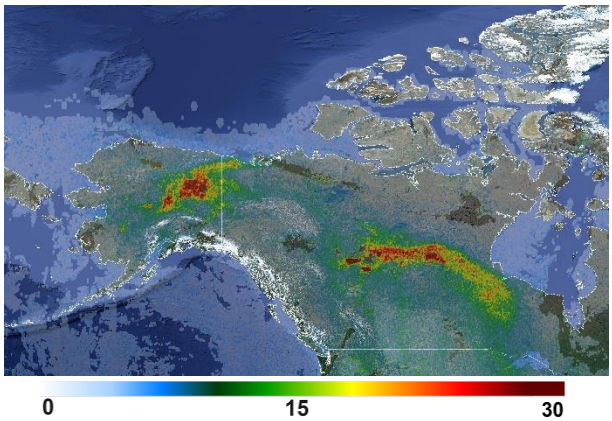

Alaska 23 Jul. 2019 (max.scale: $30x10^{15}$ molec.cm^{-2}) Alaskan wildfire emissions were particularly intense during summer 2019.

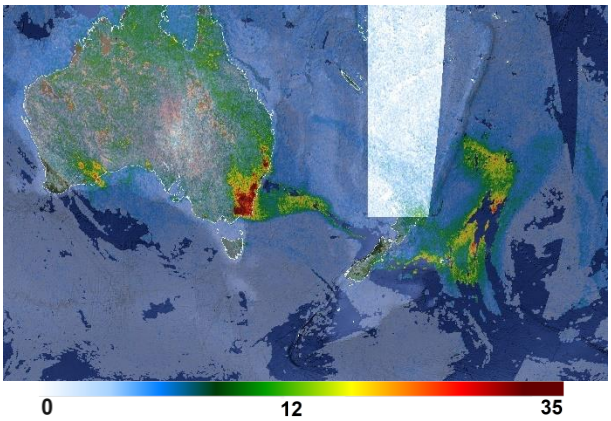

Australia 02 Jan. 2020 (max.scale: $35x10^{15}$ molec.cm^{-2}). The Australian wild fires emitted HCHO plumes that were transported as far as to the middle of the Pacific Ocean.

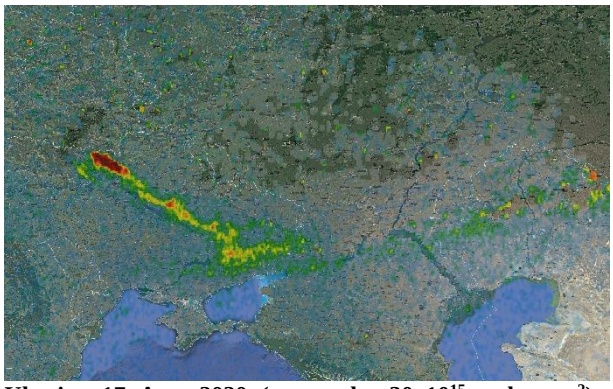

Ukraine 17 Apr. 2020 (max.scale: $30x10^{15}$ molec.cm^{-2}). Plume of HCHO caused by an important vegetation fire that occurred near Chernobyl in Ukraine.

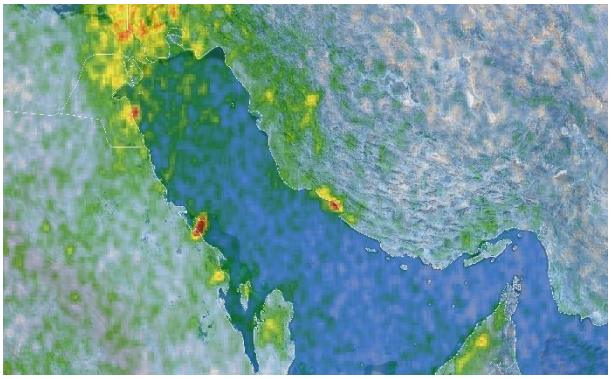

Saudi Arabia 28 Aug. 2019 (max.scale: $35x10^{15}$ molec.cm^{-2}). Pollution plume over the port of Jubail, that holds a large petrochemical hub.

Figure S2: Daily observations of TROPOMI HCHO VCD over fire events, on a spatial grid of 0.05° in latitude and longitude. Observations are filtered using the provided qa_values >0.5. Modified Copernicus Sentinel-5P satellite data, OFFL L2 HCHO product, BIRA-IASB/DLR/ESA/EU.

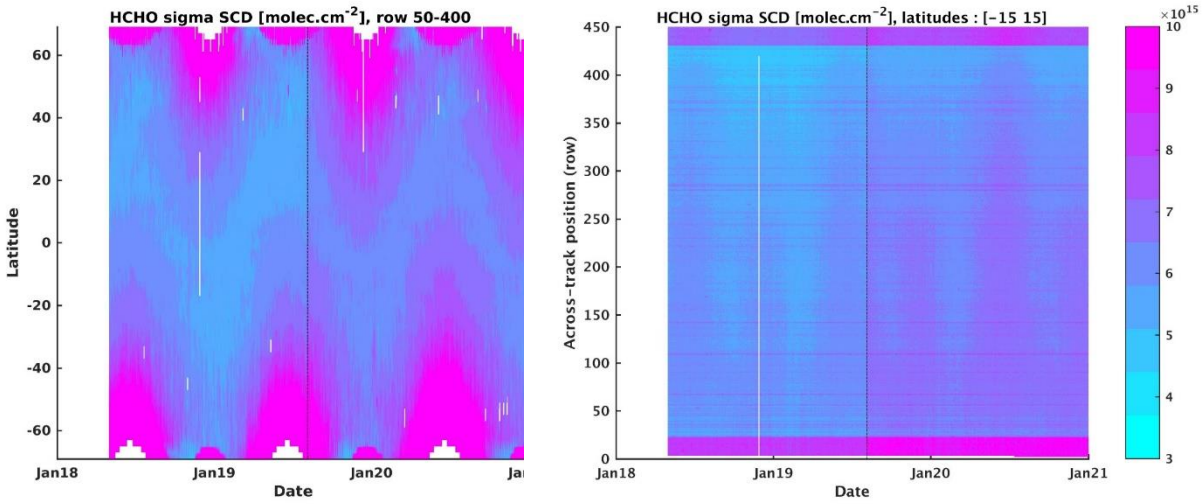

Figure S3: 1-sigma standard deviation of the OFFL TOPOMI HCHO slant columns as a function of the latitude (left column) or the detector row (right column). The step increase on 6th August 2019 reflects the change in the TROPOMI pixel size.

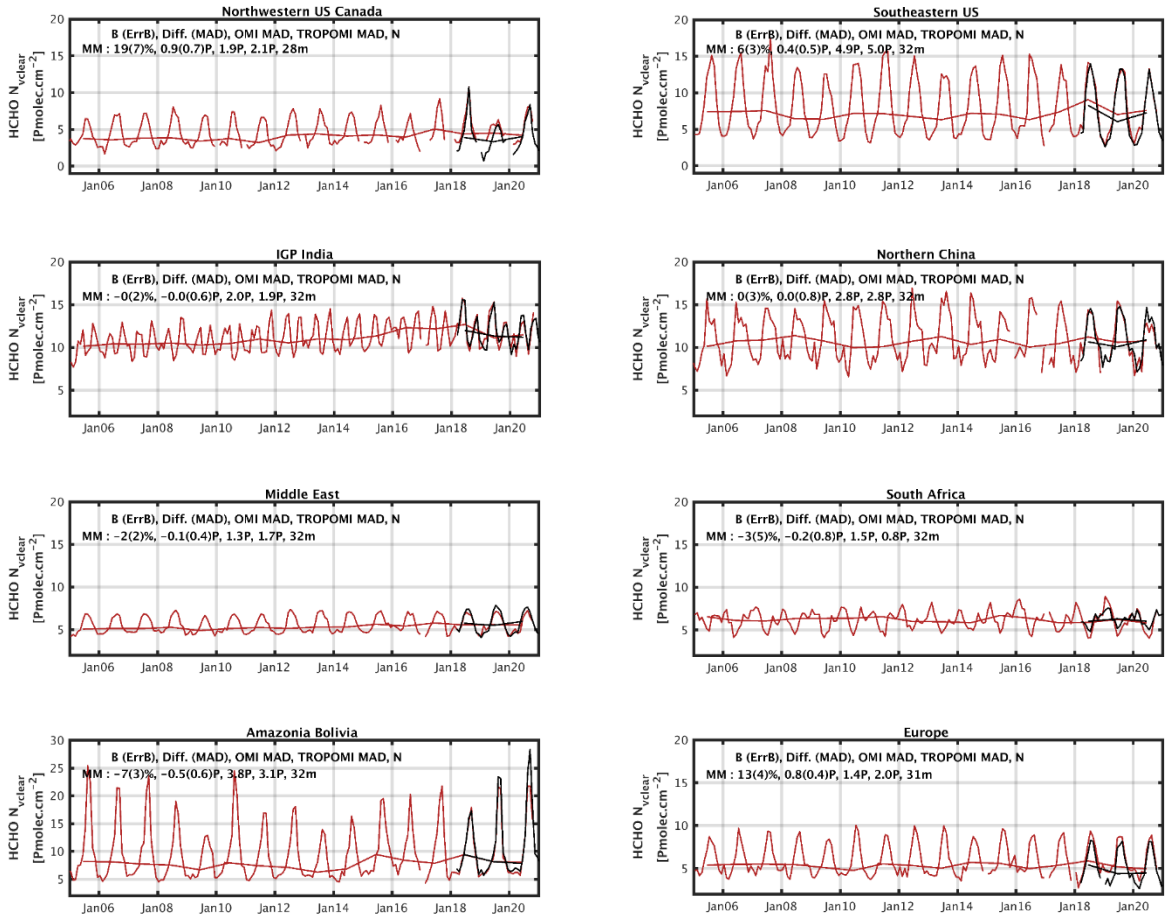

Figure S4: Monthly and yearly averaged HCHO columns (N_{v_clear}) retrieved from OMI (Oct. 2004-Dec. 2020, in red) and TROPOMI (2018-Dec.2020, in black) in a subset of the large regions selected for the comparison. [Pmolec.cm^{-2}=10^{15} molec.cm^{-2}].

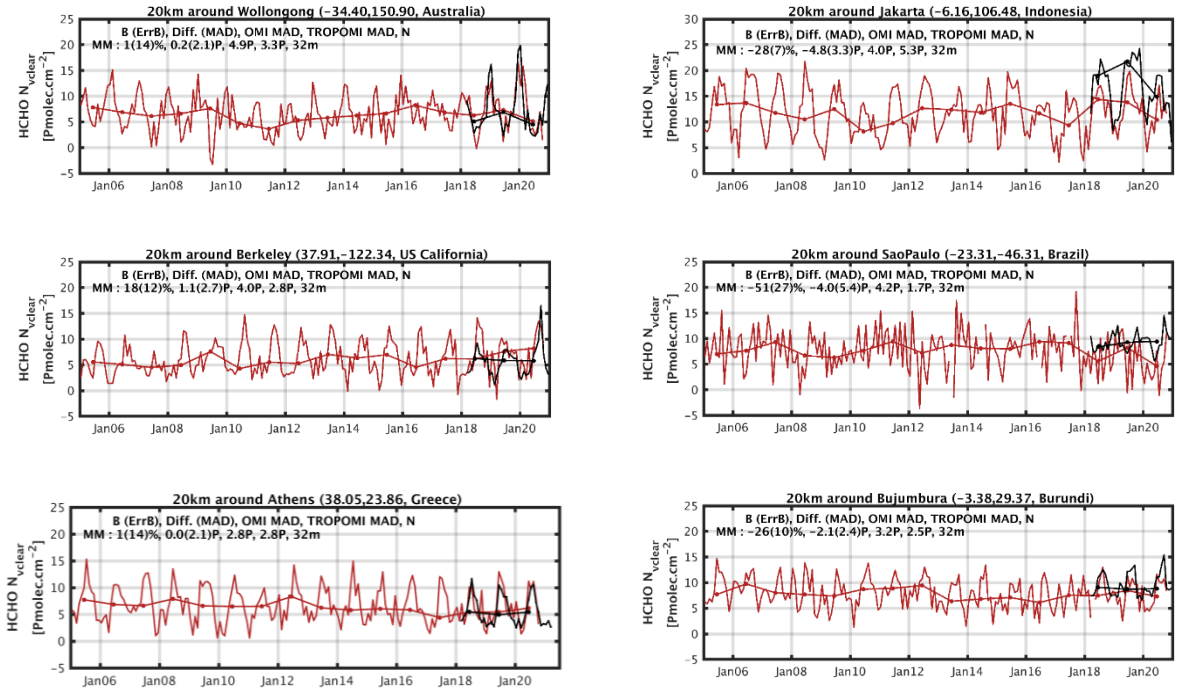

Figure S5: Monthly and yearly averaged HCHO columns (N_{v_clear}) retrieved from OMI (Oct. 2004-Dec. 2020, in red) and TROPOMI (2018-Dec. 2020, in black) in a subset of the 20-km areas selected for the comparison. [Pmolec.cm^{-2}=10^{15} molec.cm^{-2}].